

# Distributed Flexibility Characterization and Resource Allocation for Multi-zone Commercial Buildings in the Smart Grid

He Hao, Jianming Lian, Karanjit Kalsi, and Jakob Stoustrup

**Abstract**—The HVAC (Heating, Ventilation, and Air-Conditioning) system of commercial buildings is a complex system with a large number of dynamically interacting components. In particular, the thermal dynamics of each zone are coupled with those of its neighboring zones. In this paper, we study an agent-based approach to model and control commercial building HVAC system for providing ancillary services to the power grid. In the multi-agent-building-system (MABS), individual zones are modeled as agents that can communicate, interact, and negotiate with one another to achieve a common objective. We first propose a distributed characterization method on the aggregate airflow (and thus fan power) flexibility that the HVAC system can provide to the ancillary service market. A Nash-bargaining-based airflow allocation strategy is then proposed to track a dispatch signal while respecting the preference and flexibility of individual zones. Moreover, we devise a distributed algorithm to obtain the Nash bargaining solution via dual decomposition. Numerical simulations illustrate that the proposed distributed protocols are much more scalable than centralized approaches especially when the system becomes larger and more complex.

## I. INTRODUCTION

Renewable energy is “free” but at a cost of high uncertainty and variability. The vast integration of renewable energy resources into the grid creates daunting challenges for the system operator to maintain the stability and reliability of the power grid only through supply-side control. Demand-side control presents a novel and viable way to assist in managing the balance between supply and demand in the power grid. Among different demand-side resources, buildings represent about 74% of the total electricity consumption in the United States, where residential and commercial buildings respectively accounting for 38% and 36% [1], [2]. In particular, there are about 5.6 million commercial buildings, comprising 87.4 billion square feet of floorspace. The massive power consumption and enormous thermal storage enable commercial buildings as a great flexible resource for providing various grid services such as peak demand reduction [3], [4] and ancillary services [5]–[8], which are necessary to enable deep penetration of renewables.

In order to provide ancillary services to the power grid, regulating resources in most Independent System Operators (ISOs) in the United States are required to have a minimum resource size (e.g., 0.5 MW in California ISO). When a group of commercial buildings is considered for providing ancillary services, the load aggregator needs to determine the aggregate flexibility of this group and then bid into the

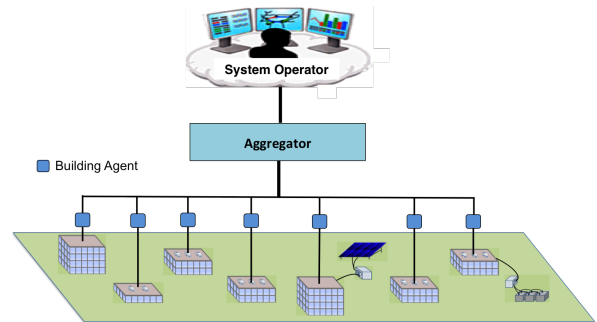


Fig. 1. Aggregation of commercial buildings for ancillary services.

ancillary service market. After the system operator collects all the bids, a co-optimization of energy and ancillary services is conducted to determine the market clearing price and the awarded capacity for each resource. In response to the grid requirements at run-time, the system operator will dispatch a grid signal (that is within the awarded capacity limit) to the load aggregator. The load aggregator then decides how to allocate the total dispatch power to different buildings, and each building is obliged to follow the allocated power signal. A schematic of using a group of commercial buildings for ancillary service provision is depicted in Fig. 1. There are two central problems to be resolved in order to enable commercial buildings participate in the ancillary service market. The first one is how to characterize the power flexibility of a multi-zone commercial building. The second one is how to control its power consumption so that it can follow a dispatch power signal while respecting the preference and comfort of individual zones.

It has been shown in [6], [9] that commercial building HVAC supply fan (which is controlled by a variable frequency drive) is a great flexible resource for providing ancillary services due to its fast and accurate responding characteristics. In [6], it has been estimated that 15% of the rated fan power can be used to follow a high-frequency regulation signal. However, this flexibility is estimated by only considering the proposed controller while requiring little change on the indoor temperature. If the allowed temperature deviation is large, the available flexibility from commercial HVAC system might be much larger. Another type of study focuses on using centralized Model Predictive Control (MPC) method to characterize the flexibility of commercial buildings and manage its energy consumption [10], [11]. Despite of its powerfulness, this kind of approach might not be scalable; it could not be migrated straightforwardly from one building to another one with a different type, structure, or size. Additionally, developing an accurate monolithic

The authors are with the Electricity Infrastructure and Buildings Division of Pacific Northwest National Laboratory, Richland, WA, 99354. Email: {He.Hao, Jianming.Lian, Karanjit.Kalsi, Jakob.Stoustrup}@pnnl.gov.

whole-building model is not a trivial task. Moreover, the computational burden becomes overwhelming for buildings with a large number of zones. On the other hand, in order to track a dispatch signal, different control strategies have been proposed for commercial buildings [6], [12], [13]. However, these approaches could not take into account the different preferences of individual thermal zones. For example, in [6], the total airflow is proportionally distributed to each zone. If the supply fan is aggressively providing ancillary service, which means the airflow change from baseline is relatively large, the proportional allocation strategy might not be fair, and respect each zone's preference and flexibility.

To tackle the above challenges, we propose in this paper a scalable, distributed flexibility characterization method for multi-zone commercial buildings, and a fair, and efficient bargain-based airflow allocation strategy to respect the preference and flexibility of each zone. We first study an agent-based approach to model multi-zone commercial buildings. In this multi-agent-building-system, each zone is modeled as an agent, and we design distributed coordination protocols to enable them to interact and negotiate locally while achieving a global objective. There are many benefits of modeling a commercial building as a multi-agent-system. First, zonal dynamics are easy to develop and calibrate. Second, it is flexible, modular, and scalable. The proposed method can be easily applied to heterogeneous buildings. Third, it allows each zone to be more adaptive to structure change, external disturbances, and setting adjustment. Moreover, compared to centralized flexibility characterization approaches, our approach relies on that each zone characterizing its own flexibility based on local information, and thus, the modeling and computational complexities are much lower.

We next propose a Nash-bargaining-based cooperative airflow allocation strategy for multi-zone commercial buildings. The Nash Bargaining Solution (NBS) is an attractive approach for solving cooperative resource allocation problems as it balances fairness and efficiency [14]. Unlike non-cooperative game-theoretic approaches in which agents make decisions independently and selfishly, NBS is a unique, and Pareto-efficient solution that enables agents to collaboratively make decisions to maximize the social welfare. Moreover, using dual decomposition, a distributed bargaining protocol is developed for individual zones to cooperatively reach the optimal airflow allocation, while respecting the preference and flexibility of each zone.

The remainder of this paper unfolds as follows. In Section II, we study an agent-based modeling approach for multi-zone commercial building HVAC system. Distributed flexibility characterization and resource allocation strategies are proposed in Section III and Section IV respectively. Section V is devoted to numerical experiments. The paper ends with conclusions and future work in Section VI.

## II. AGENT-BASED MODELING OF MULTI-ZONE COMMERCIAL BUILDINGS

The configuration of a typical multi-zone commercial building HVAC system is depicted in Fig. 2. In this section,

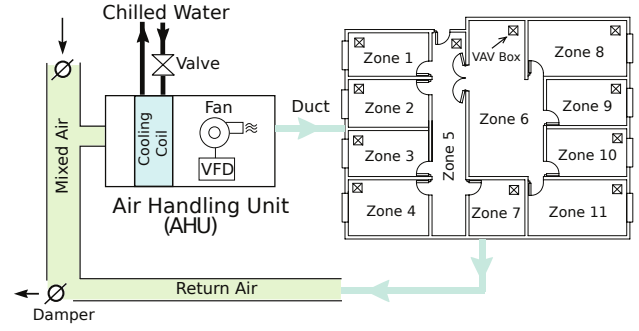


Fig. 2. Schematic of a typical commercial building HVAC system that serves 11 zones.

we study an agent-based modeling approach for multi-zone commercial buildings.

*Definition 1: A Multi-Agent-Building-System (MABS)* refers to a multi-zone commercial building, in which each thermal zone is modeled as an agent. Their interaction topology is described by an information graph  $\mathcal{G} = (\mathcal{N}, \mathcal{E})$  with nodes (zones or agents) set  $\mathcal{N} = \{1, \dots, n\}$  and edge set  $\mathcal{E} \subset \mathcal{N} \times \mathcal{N}$ . An edge  $(i, j)$  exists if zone  $i$  and zone  $j$  are physically adjacent. The set of neighbors of zone  $i$  is denoted as  $\mathcal{N}_i := \{j \in \mathcal{N} : (i, j) \in \mathcal{E}\}$ .  $\square$

The thermal dynamic model of a  $n$ -zone building can be constructed by interconnection of a network of Resistance-Capacitance (RC) models of individual zones [6], [15], [16]. The thermal dynamics of the  $i^{\text{th}}$  zone ( $i \in \mathcal{N}$ ) are described by the following RC model:

$$C^i \frac{dT^i(t)}{dt} = \frac{T_o - T^i(t)}{R^i} + \sum_{j \in \mathcal{N}_i} \frac{T^{(i,j)}(t) - T^i(t)}{R^{(i,j)}} + c_p m^i(t) (T_s^i(t) - T^i(t)) + Q^i(t), \quad (1a)$$

$$C^{(i,j)} \frac{dT^{(i,j)}(t)}{dt} = \frac{T^i(t) - T^{(i,j)}(t)}{R^{(i,j)}} + \frac{T^j(t) - T^{(i,j)}(t)}{R^{(i,j)}}, \quad (1b)$$

where the variables and parameters, as well as their units, are described in Table I. The first term  $\frac{1}{R^i}(T_o - T^i)$  on the RHS (Right Hand Side) of (1a) represents the heat conduction between zone  $i$  and the outside environment, the second term  $\sum_{j \in \mathcal{N}_i} \frac{1}{R^{(i,j)}}(T^{(i,j)} - T^i)$  describes the heat exchange between zone  $i$  and its surrounding inside walls that separate itself from neighboring zones, the third term  $c_p m^i(T_s^i - T^i)$  denotes the heat removal by the air conditioner, and the last term  $Q^i$  is the heat gain from reheating, solar, occupants, lights, etc. Similarly, the first term  $\frac{1}{R^{(i,j)}}(T^i - T^{(i,j)})$  on the RHS of (1b) represents the heat exchange between zone  $i$  and the wall separating zone  $i$  and zone  $j$ , and the second term  $\frac{1}{R^{(i,j)}}(T^j - T^{(i,j)})$  denotes the heat exchange between zone  $j$  and the wall separating zone  $i$  and zone  $j$ .

In this paper, we consider the supply fan as the only source of flexibility for ancillary services provision, as in [6], [9], [17]. The supply fan is one of the most important components in the HVAC system. Like a heart that pumps blood through a human body, the fan distributes the supply air (usually at 12.8°C) throughout the building over ducts. The power consumption of the supply fan is approximately proportional to the cube of its supply airflow [17], [18],

$$P(t) = c(m(t))^3, \quad (2)$$

TABLE I  
DESCRIPTION OF PARAMETERS OF BUILDING THERMAL DYNAMICS

Parameter	Description	Unit
$T^i$	zone $i$ 's indoor temperature	$^{\circ}\text{C}$
$T^{(i,j)}$	inside temperature of the wall that separates zone $i$ and zone $j$	$^{\circ}\text{C}$
$C^i$	zone $i$ 's thermal capacitance	$\text{J}/^{\circ}\text{C}$
$C^{(i,j)}$	thermal capacitance of the wall that separates zone $i$ and zone $j$	$^{\circ}\text{C}/\text{W}$
$R^i$	thermal resistance of the wall that separates zone $i$ and outside	$^{\circ}\text{C}/\text{W}$
$R^{(i,j)}$	thermal resistance of the wall that separates zone $i$ and zone $j$	$^{\circ}\text{C}/\text{W}$
$m^i$	zone $i$ 's supply airflow	$\text{kg}/\text{s}$
$T_s^i$	zone $i$ 's supply air temperature	$^{\circ}\text{C}$
$T^{i,*}$	zone $i$ 's temperature setpoint	$^{\circ}\text{C}$
$c_p$	specific heat of air	$\text{J}/\text{g}/^{\circ}\text{C}$
$T_o$	outside air temperature	$^{\circ}\text{C}$
$Q^i$	zone $i$ 's heat gain from reheating, solar, etc.	$\text{W}$

where  $c$  is a constant, and  $m(t) = \sum_{i \in \mathcal{N}} m^i(t)$  is the total supply airflow. As a result, given a value of the fan power, it can be straightforwardly translated to the corresponding supply airflow, and vice versa.

In this paper, we study two central problems that enable buildings to provide ancillary services to the grid: (1) characterization/quantification of the fan power (and thus supply airflow) flexibility that can be offered to the grid, (2) optimal allocation of the supply airflow to track a dispatched fan power signal, while respecting the preference and flexibility of each zone.

### III. DISTRIBUTED FLEXIBILITY CHARACTERIZATION

In this section, we study characterization of the aggregate airflow flexibility of a multi-zone commercial building. In particular, we aim to quantify the maximum, minimum, and the baseline airflow requirements in a considered time horizon, while maintaining the indoor temperature of each zone within a user-specified range. Recently, Model Predictive Control (MPC) has become a popular tool for building operation and control [11], [19]. However, for a large commercial building with many zones, the number of variables and constraints becomes inhibitably large, which makes it challenging to use a *centralized* MPC-based approach to characterize the airflow flexibility. Furthermore, the centralized characterization approach is not scalable, since it strongly depends on the whole-building model, and it cannot be easily migrated from one building to another one with a different structure, configuration, or size.

To this end, we propose a multi-agent-based distributed airflow flexibility characterization method. This multi-agent-based approach represents a natural problem decomposition, and is able to find innovative solutions by enabling agents to interact locally to achieve a global objective. In the MABS, each zone (agent) utilizes MPC to characterize its own flexibility only based on its own zonal dynamics, and treats the temperatures of its neighbors as exogenous variables, which can be obtained by iteratively communicating with its neighboring zones.

We consider a discrete time system, and use  $t$  to index the

current time step. The thermal model of each zone can be written compactly in the following discrete form

$$T_{t+1}^i = f^i(T_t^i, u_t^i, w_t^i),$$

where the input  $u_t^i \in \mathbb{R}$  is the supply airflow rate  $m_t^i$ , and the disturbance vector  $w_t^i = [Q_t^i, T_{o,t}, T_t^{j \in \mathcal{N}_i}] \in \mathbb{R}^{2+|\mathcal{N}_i|}$  contains the zonal heat gain, the outside air temperature, and the temperatures of neighboring zones. In this paper, we assume there are  $K$  time steps in each prediction horizon, and we use  $k \in \mathcal{K} = \{0, 1, \dots, K-1\}$  to index the  $k^{\text{th}}$  step. For each zone, we aim to characterize the minimum and maximum airflow requirements in the prediction horizon to maintain its zone temperature within the user-specified temperature band.

We first consider characterization of the minimum airflow over the prediction horizon. More specifically, for each  $i \in \mathcal{N}$ , we estimate its minimum airflow,  $\{\underline{m}_{t+k}^i\}_{k \in \mathcal{K}}$ , using the following algorithm<sup>1</sup>:

$$\min_{m_{t \rightarrow t+k-1}^i} \sum_{k=0}^{K-1} \omega_{t+k}^i m_{t+k}^i \quad (3a)$$

$$\text{subject to: } T_{t+k+1}^i = f^i(T_{t+k}^i, u_{t+k}^i, w_{t+k}^i), \quad \forall k \in \mathcal{K}, \quad (3b)$$

$$T_{t+k}^{i,-} \leq T_{t+k}^i \leq T_{t+k}^{i,+}, \quad \forall k \in \mathcal{K}, \quad (3c)$$

$$m_{t+k}^{i,-} \leq m_{t+k}^i \leq m_{t+k}^{i,+}, \quad \forall k \in \mathcal{K}, \quad (3d)$$

$$T_{t+K}^{i,-} \leq T_{t+K}^i \leq T_{t+K}^{i,+}, \quad (3e)$$

where  $\omega_{t+k}^i$  is a non-negative weight negotiating the importance of  $m_{t+k}^i$  at time step  $t+k$ , and satisfies  $\sum_{k \in \mathcal{K}} \omega_{t+k}^i = 1$ . Additionally,  $T_{t+k}^{i,-}$  and  $T_{t+k}^{i,+}$  are respectively the lower and upper temperature bounds at time step  $t+k$ . Moreover,  $m_{t+k}^{i,-}$  is the minimum airflow that is imposed to guarantee a minimal ventilation level, and  $m_{t+k}^{i,+}$  is the maximum airflow limited by the size of the VAV box. Similarly, we characterize the maximum airflow,  $\{\overline{m}_{t+k}^i\}_{k \in \mathcal{K}}$ , using the following algorithm:

$$\max_{m_{t \rightarrow t+k-1}^i} \sum_{k=0}^{K-1} \omega_{t+k}^i m_{t+k}^i \quad (4a)$$

$$\text{subject to: } T_{t+k+1}^i = f^i(T_{t+k}^i, u_{t+k}^i, w_{t+k}^i), \quad \forall k \in \mathcal{K}, \quad (4b)$$

$$T_{t+k}^{i,-} \leq T_{t+k}^i \leq T_{t+k}^{i,+}, \quad \forall k \in \mathcal{K}, \quad (4c)$$

$$m_{t+k}^{i,-} \leq m_{t+k}^i \leq m_{t+k}^{i,+}, \quad \forall k \in \mathcal{K}, \quad (4d)$$

$$T_{t+K}^{i,-} \leq T_{t+K}^i \leq T_{t+K}^{i,+}. \quad (4e)$$

However, for each zone  $i \in \mathcal{N}$ , the above characterizations rely on the temperature profiles of its neighboring zones in the prediction horizon, i.e.,  $\{T_{t+k}^j\}_{k \in \mathcal{K}, j \in \mathcal{N}_i}$ . In turn, zone  $i$ 's temperature evolution  $\{T_{t+k}^i\}_{k \in \mathcal{K}}$  also impacts the characterizations of its neighbors. Upon observing this coupling relationship, we propose in this paper a distributed iterative characterization approach. At the initial step, for each zone  $i \in \mathcal{N}$ , we assume the temperatures of its neighboring zones in the prediction horizon is the same as their respective current temperature, i.e.,  $T_{t+k}^j = T_t^j$  for all  $k \in \mathcal{K}$ , and  $j \in$

<sup>1</sup>We comment that additional constraints can be added to customize the characterization. For example, if the minimum airflow in the prediction horizon are required to be equal, then constraint  $m_{t+k}^i = m_{t+l}^i$  for all  $k, l \in \mathcal{K}$  can be imposed.

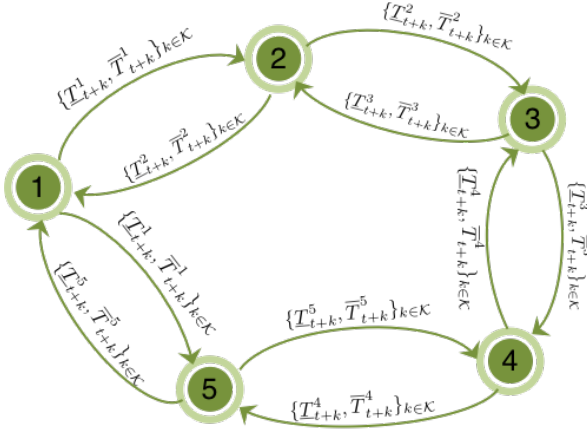


Fig. 3. Information exchange during distributed flexibility characterization.

$\mathcal{N}_i$ . Next, we use algorithms (3) and (4) to characterize the airflow flexibility of each zone. At the same time, we obtain its temperature profiles from (3) and (4), and denote them as  $\{\underline{T}_{t+k}^i\}_{k \in \mathcal{K}}$  and  $\{\bar{T}_{t+k}^i\}_{k \in \mathcal{K}}$  respectively. These temperature profiles are then communicated to its neighboring zones (see Fig. 3 for an illustrating example). With these updated temperature profiles, each zone characterizes its airflow flexibility and obtain new temperature profiles. We repeat the above process until the downward and upward airflow flexibility of each zone converges. The distributed iterative airflow characterization method is given in Algorithm 1. Note that this algorithm is fully distributed; it can be executed in a parallel manner.

#### Algorithm 1 Distributed Flexibility Characterization Method

**Require:**  $\varepsilon$ ;

- 1: assign  $\underline{m}_{t+k}^i = 0, \bar{m}_{t+k}^i = 0$ ;
- 2: **repeat**
- 3:   **for**  $i=1:n$  **do**
- 4:     assign  $\underline{M}_{t+k}^i = \underline{m}_{t+k}^i, \bar{M}_{t+k}^i = \bar{m}_{t+k}^i, \forall k \in \mathcal{K}$ ;
- 5:     get  $\{\underline{T}_{t+k}^j, \bar{T}_{t+k}^j\}_{k \in \mathcal{K}, j \in \mathcal{N}_i}$  from neighbors;
- 6:     characterize  $\{\underline{m}_{t+k}^i, \bar{m}_{t+k}^i\}_{k \in \mathcal{K}}$  using (3) and (4);
- 7:     obtain  $\{\underline{T}_{t+k}^i, \bar{T}_{t+k}^i\}_{k \in \mathcal{K}}$  from (3) and (4);
- 8:     transmit new temperature profiles to its neighbors;
- 9:   **end for**
- 10: **until**  $\max_i (\|\underline{M}_{t+k}^i - \underline{m}_{t+k}^i\| + \|\bar{M}_{t+k}^i - \bar{m}_{t+k}^i\|) \leq \varepsilon$
- 11: **return**  $\{\underline{m}_{t+k}^i, \bar{m}_{t+k}^i\}_{k \in \mathcal{K}}$  for all  $i$ ;

Moreover, we use a similar iterative distributed MPC approach to predict the baseline airflow and fan power. In particular, each zone executes the following algorithm and exchange temperature profiles with its neighboring zones to characterize its baseline airflow in the prediction horizon,

$$\min_{m_{t \rightarrow t+k-1}^i} \sum_{k=0}^{K-1} ((T_{t+k}^i - T_{t+k}^{i,*})^2 + \omega^i m_{t+k}^i) \quad (5a)$$

$$\text{subject to: } T_{t+k+1}^i = f^i(T_{t+k}^i, u_{t+k}^i, w_{t+k}^i), \quad \forall k \in \mathcal{K}, \quad (5b)$$

$$m_{t+k}^{i,-} \leq m_{t+k}^i \leq m_{t+k}^{i,+}, \quad \forall k \in \mathcal{K}, \quad (5c)$$

where  $T_{t+k}^{i,*}$  is the desired temperature of Zone  $i$  at time step  $t+k$ , and  $\omega^i$  is a non-negative weighting parameter balancing

temperature tracking error and energy saving. After convergence from iterations, the obtained solution  $\{m_{t+k}^{i,*}\}_{k \in \mathcal{K}}$  is the baseline airflow of Zone  $i$  in the predicted horizon. As a result, the baseline fan power is given by  $\{P_{t+k}^*\}_{k \in \mathcal{K}}$ , where  $P_{t+k}^* = c(\sum_i m_{t+k}^{i,*})^3$ . The baseline fan power will be served as a basis compared to which the HVAC system determines how much more or less power to consume in order to track a dispatched grid signal. If the actual power consumption is greater than the baseline, it “absorbs” power from the grid; if it is smaller, it “discharges” power to the grid. This makes building behave as a virtual storage to absorb the uncertainty of the grid.

*Definition 2:* The aggregate airflow flexibility from all zones is defined as a set of airflow trajectories,  $\{m_{t+k}\}_{k \in \mathcal{K}}$ , such that

$$\mathcal{F}_t = \{m_{t+k}, \forall k \in \mathcal{K} \mid \sum_i \underline{m}_{t+k}^i \leq m_{t+k} \leq \sum_i \bar{m}_{t+k}^i\}.$$

Correspondingly, the aggregate fan power flexibility that can be offered to the grid is defined as

$$\mathcal{P}_t = \{P_{t+k}, \forall k \in \mathcal{K} \mid \underline{P}_{t+k} \leq P_{t+k} \leq \bar{P}_{t+k}\}.$$

where  $\underline{P}_{t+k} = c(\sum_i \underline{m}_{t+k}^i)^3$  and  $\bar{P}_{t+k} = c(\sum_i \bar{m}_{t+k}^i)^3$ .  $\square$

The upward flexibility  $\{\bar{P}_{t+k} - P_{t+k}^*\}_{k \in \mathcal{N}}$  and downward flexibility  $\{P_{t+k}^* - \underline{P}_{t+k}\}_{k \in \mathcal{N}}$  are the capacities that can be bid into the ancillary service market.

So far, we have characterized the fan power flexibility that a multi-zone commercial building can offer to the grid. However, given a dispatch power profile  $\{P_{t+k}\}_{k \in \mathcal{K}} \in \mathcal{P}_t$ , the question of how to allocate the supply airflow so that the fan power consumption tracks the dispatch signal while respecting the flexibility of each zone is not answered. Moreover, different zones in a commercial building have different preferences or priorities. For instance, the indoor air quality requirement of a laboratory zone might be more stringent than a cafeteria zone. Therefore, the allocation of supply airflow must respect the flexibility as well as the preference of each zone. We propose in next section a bargaining-based distributed airflow allocation strategy to achieve the above objectives.

#### IV. BARGAIN-BASED AIRFLOW ALLOCATION STRATEGY

In this paper, we study a single-stage airflow allocation problem, which only focuses on the current time step  $t$ . Bargaining is a process in which players achieve interim settlements step-by-step, where each settlement is a starting point for further negotiations. Let  $\mathbf{S} \in \mathbb{R}^n$  be a convex and compact set comprising all the outcomes of a bargain, and  $\mathbf{d} = (d^1, \dots, d^n) \in \mathbb{R}^n$  be the disagreement points that are assigned to the players if a bargain (negotiation) is not successful.

*Definition 3:* A bargaining solution is a mapping  $\mathcal{B} : \mathcal{S} \rightarrow \mathbb{R}^n$ . We call a bargaining solution  $\mathbf{q} = (q^1, \dots, q^n) \in \mathbf{S}$  is *Pareto-efficient* if there does not exist a solution  $\bar{\mathbf{q}} = (\bar{q}^1, \dots, \bar{q}^n) \in \mathcal{S}$  such that

$$u^i(\bar{q}^i) \geq u^i(q^i), \quad \forall i \in \mathcal{N},$$

where  $u^i$  is the utility function of player  $i$ . A bargaining solution  $\mathbf{q} \in \mathcal{S}$  is called  $\epsilon$  Pareto-efficient if

$$\|u^i(q^i) - u^i(\bar{q}^i)\| \leq \epsilon, \quad \forall i \in \mathcal{N},$$

where  $\bar{\mathbf{q}} \in \mathcal{S}$  is a Pareto-efficient solution, and  $\epsilon$  is a small positive number.  $\square$

Consider a  $n$ -zone commercial building bargaining over allocating a dispatched total supply airflow  $m_t^*$ . Each zone has airflow requirement  $m_t^i \in [\underline{m}_t^i, \bar{m}_t^i]$ , where  $\underline{m}_t^i, \bar{m}_t^i$  are respectively the minimum and maximum airflow requirements of Zone  $i$  at time step  $t$ . With a change of variable,  $q_t^i = (m_t^i - \underline{m}_t^i) / (\bar{m}_t^i - \underline{m}_t^i)$ , we scale the airflow requirement of each zone so that  $q_t^i \in [0, 1]$  for all  $i \in \mathcal{N}$ . The preference of each zone at time step  $t$  is modeled by a utility function  $u_t^i(q_t^i) : [0, 1] \rightarrow \mathbb{R}_+$  with airflow allocation  $q_t^i$ . In this paper, we assume each utility function is concave, differentiable, and  $u_t^i(q_t^i) = 0$  if  $q_t^i = 0$ .

From a game theoretic perspective, each player in a negotiation must always keep in mind that a strategy of trying to unilaterally improve its own return at the expense of the other players will typically be self-defeating [20]. Therefore, we consider a cooperative game, in which each zone is motivated to negotiate with others in a collaborative way to jointly maximize their utility functions. To solve the airflow allocation problem, we consider the Nash Bargaining Solution (NBS) concept. Formally, the Nash bargaining problem is formulated as

$$\max_{q_t^i\text{'s}} \prod_{i=1}^n u_t^i(q_t^i) \quad (6a)$$

$$\text{subject to: } \sum_{i=1}^n \underline{m}_t^i + (\bar{m}_t^i - \underline{m}_t^i)q_t^i = m_t^*, \quad (6b)$$

$$0 \leq q_t^i \leq 1, \quad \forall i \in \mathcal{N}, \quad (6c)$$

where the objective function is referred to as the Nash product. Additionally, we have assumed the disagreement points to be zero. The solution to the Nash bargaining problem (6) is a fair and Pareto-efficient allocation that satisfies the four axioms of Nash [14]. However, no bargaining procedure was given to tell agents how to bargaining among themselves to reach the Nash bargaining solution. Moreover, 70% of the commercial buildings in the United States don't have building automation systems (BASs) that can be used to solve the Nash bargaining problem (6). Therefore, a distributed protocol is strongly preferred to enable zones to compute and interact locally to reach the Nash bargaining solution.

To this end, we propose in this paper a distributed bargaining protocol for zones to negotiate among themselves to reach the optimal airflow allocation [21]. Since the utility functions are concave and non-negative, the Nash bargaining solution to (6) is equivalent to that of the following convex optimization problem,

$$\max_{q_t^i\text{'s}} f(q_t^1, \dots, q_t^n) = \sum_{i=1}^n \log(u_t^i(q_t^i)) \quad (7a)$$

$$\text{subject to: } \sum_{i=1}^n \underline{m}_t^i + (\bar{m}_t^i - \underline{m}_t^i)q_t^i = m_t^*, \quad (7b)$$

$$0 \leq q_t^i \leq 1, \quad \forall i \in \mathcal{N}. \quad (7c)$$

Upon observing the separability of the cost function and constraints, our insight is to take advantage of the dual decomposition technique. Following straightforward algebra from [22], [23], it can be shown that the optimal solution of (7) can be obtained by using the following iterative procedure. First of all, we broadcast an initial value  $\lambda_0$  of the dual variable to all zones. Each zone then locally solves the following convex optimization problem

$$\max_{q_t^i} g^i(\lambda_k) = \log u_t^i(q_t^i) - \lambda_k m_t^i \quad (8a)$$

$$\text{subject to: } 0 \leq q_t^i \leq 1, \quad \forall i \in \mathcal{N}, \quad (8b)$$

where  $m_t^i = \underline{m}_t^i + (\bar{m}_t^i - \underline{m}_t^i)q_t^i$ . The dual variable is then updated locally using the following gradient decent algorithm

$$\lambda_{k+1}^i = \lambda_k^i - \gamma s_k^i, \quad (9a)$$

$$s_k^i = m_t^* - \sum_{i=1}^n (\underline{m}_t^i + (\bar{m}_t^i - \underline{m}_t^i)q_t^{i,*}), \quad (9b)$$

where  $\gamma > 0$  is an appropriately small step size, and  $q_t^{i,*}$  is the optimal solution of (8). We repeat (8)-(9) until convergence is achieved, i.e.,  $\max_i \|s_k^i\| \leq \epsilon$  for a small positive number  $\epsilon$ . The iterative gradient decent algorithm is summarized in Algorithm 2.

---

#### Algorithm 2 Distributed Nash Bargaining Protocol

---

**Require:**  $\epsilon, m_t^*$ , and  $\lambda_0$ ;

1: assign  $k = 0$ ;

2: **repeat**

3:   **for**  $i=1:n$  **do**

4:     solve optimization problem (8);

5:     update subgradient  $s_k^i$  using (9);

6:     assign  $k = k + 1$ ;

7:   **end for**

8: **until**  $\max_i \|s_k^i\| \leq \epsilon$

9: **return**  $q_t^{i,*}$  for all  $i \in \mathcal{N}$ ;

---

*Remark 1:* The above iterative process describes a bargaining/negotiation process for zones to allocate a dispatched total airflow. Given an initial "price"  $\lambda_0$  on the airflow, each zone evaluates its own interest by solving (8), and bargaining for a new allocation  $m_t^{i,*} = \underline{m}_t^i + (\bar{m}_t^i - \underline{m}_t^i)q_t^{i,*}$ . They then jointly propose a new allocation proposal  $(m_t^{1,*}, \dots, m_t^{n,*})$ . If there is still airflow surplus, i.e.,  $s_k > 0$ , then a new price is constructed using (9), and zones repeat the previous bargaining process. This process is repeated until all zones are satisfied with their current proposals or there is no more airflow surplus. It is interesting to see that the above procedure also describes a non-cooperative game, in which agents independently and selfishly maximize their own benefits, which are defined by the difference between the scaled preference,  $\log u_t^i(q_t^i)$ , and the cost of airflow consumption,  $\lambda_k m_t^i$  [24]. The cooperative and non-cooperative bargaining games have intimate relationship: the non-cooperative game serves as a procedure to obtain the cooperative result, while the cooperative bargaining solution serves as the non-cooperative equilibrium [25].  $\square$



## V. NUMERICAL EXPERIMENTS

In this section, we compare our proposed distributed flexibility characterization and resource allocation methods with centralized approaches, and demonstrate the efficacy and scalability of our distributed methods.

### A. Centralized Airflow Flexibility Characterization

In this section, we first consider a centralized MPC approach as a benchmark to characterize the airflow flexibility of multi-zone commercial buildings. The thermal model (1) of a multi-zone building can be written compactly as

$$x_{t+1} = f(x_t, u_t, w_t), \quad (10)$$

where the state vector  $x_t = [T^1(t), \dots, T^n(t), T^{(i,j)}(t)'s] \in \mathbb{R}^{n+m}$  collects the temperatures of  $n$  zones and  $m$  separating walls, the input vector  $u_t = [m^1(t), \dots, m^n(t)] \in \mathbb{R}^n$  collects the airflow into each zone, and the disturbance vector  $w_t = [Q^1(t), \dots, Q^n(t), T_o(t)] \in \mathbb{R}^{n+1}$  contains the heat gain of each zone, and the outside air temperature.

We first use the following algorithm to characterize the minimum airflow requirement of the HVAC system in the prediction horizon,

$$\min_{u_{t \rightarrow t+N}} J_t(x_t, u_{t \rightarrow t+N}) = \sum_{k=0}^{N-1} \omega_{t+k} m_{t+k} \quad (11a)$$

$$\text{subject to: } x_{t+k+1} = f(x_t, u_t, w_t), \quad \forall k \in \mathbb{K}, \quad (11b)$$

$$u_{t+k} \in \mathcal{U}_{t+k}, \quad \forall k \in \mathbb{K}, \quad (11c)$$

$$x_{t+k} \in \mathcal{X}_{t+k}, \quad \forall k \in \mathbb{K}, \quad (11d)$$

$$x_{t+K} \in \mathcal{X}_{t+K}, \quad (11e)$$

where  $\omega_{t+k}$ 's are non-negative weights negotiating the importance of  $m_{t+k}$ 's at different time steps, and  $\mathcal{X}_{t+k}$ ,  $\mathcal{U}_{t+k}$  are respectively the feasible sets of the systems states  $x_{t+k}$  and control inputs  $u_{t+k}$  at time step  $t+k$ , which are determined by user specified temperature band, and operational constraints on the airflow. Similarly, we characterize the maximum airflow requirements by maximizing the objective function in (11). For such a centralized characterization approach, at each time step, there are  $(n+m) \times (K+1)$  state variables,  $n \times K$  decision variables, and  $(n+m) \times K + n \times K \times 2 + n \times K \times 2 + n \times 2$  constraints. The computational burden and communicational requirements are overwhelming when the number of zones in the building is large and their interconnection is complex.

**Numerical Example:** We numerically compare the distributed and centralized airflow flexibility characterization methods. The thermal models used in the simulations are the same as those used in [6]. We discretize the thermal dynamics by a sample time of 5 minutes, and predict the airflow flexibility for the next 6 time steps, which is 30 minutes. The distributed algorithm (Algorithm 1) and the centralized algorithm (11) are both solved using YALMIP toolbox [26] in MATLAB<sup>®</sup> on a Macintosh PC with Yosemite operating system, 3.4 GHz Intel core i5 processor, and 16 GB 1600 MHz DDR3 memory. We observe from Fig. 4 that the characterized airflow flexibility using the distributed and centralized characterization methods are the same. However,

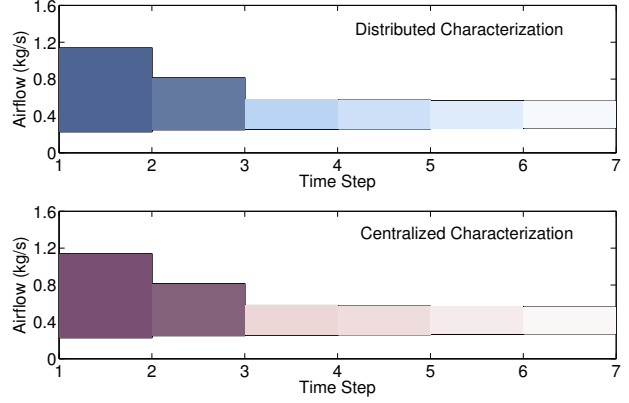


Fig. 4. Comparison of the characterized airflow flexibility between the distributed and centralized characterization methods.

the computational time using the distributed characterization method is about 10 seconds, and it is much smaller than that using the centralized characterization method, which is about 100 seconds.

### B. Raiffa Bargaining Protocol

We also consider a Raiffa bargaining procedure for airflow allocation as a benchmark for comparison [27]. The Raiffa bargaining protocol is a simple and straightforward step-by-step bargaining procedure with each player repeating the calculations of its own *ideal point* and *middle point* until an  $\epsilon$  Pareto-efficient solution is reached.

*Definition 4:* The *ideal point* of player  $i$  is defined as

$$I^i = \arg \max_{q^i} \{u^i(q^i) | \mathbf{q} \in \mathcal{S}, u^j(q^j) = u^j(d^j), \forall j \in \mathcal{N} \setminus i\}.$$

It is obtained by maximizing its own utility function while making the other players' utilities the same as those that using their disagreement points. The *middle point* of player  $i$  is defined as

$$\mu^i = \frac{1}{n} I^i + \left(1 - \frac{1}{n}\right) d^i = d^i + \frac{I^i - d^i}{n}.$$

It is obtained by “sharing the resource surplus evenly among all the players”. The middle point will serve as the disagreement point in the next bargaining iteration.  $\square$

The detailed bargaining protocol is described in Algorithm 3. Additionally, it is shown in [27] that the Raiffa bargaining solution yields an  $\epsilon$  Pareto-efficient solution after a sufficiently large number of iterations of bargains.

**Numerical Example:** In this section, we assume the utility function of each zone is given by a power function

$$u_t^i = (q_t^i)^{\alpha_t^i}, \quad (12)$$

where the power coefficient  $\alpha_t^i$  that satisfies  $0 \leq \alpha_t^i \leq 1$  measures the degree of risk aversion of zone  $i$ . In a bargaining game, players with larger degrees of risk aversion will obtain larger share of the resource. In allocating the airflow, we use the power coefficient  $\alpha_t^i$  to measure the importance/priority of zone  $i$  at time step  $t$ . For example, if zone  $i$  is an occupied laboratory, it will be assigned with

---

**Algorithm 3** Discrete Raiffa Bargaining Protocol
 

---

**Require:**  $d_0$  and  $\epsilon$ 

```

1: assign  $k = 0$ ;
2: repeat
3:   for  $i=1:n$  do
4:     compute  $I_k^i$ ;
5:     compute  $\mu_k^i = I_k^i + (1 - \frac{1}{n})d_{k-1}^i$ ;
6:     assign  $d_k^i = \mu_k^i$ ;
7:      $k = k + 1$ ;
8:   end for
9: until  $\max_j \|\mu_k^j - \mu_{k-1}^j\| \leq \epsilon$ 
10: return  $\mu_k = (\mu_k^1, \dots, \mu_k^n)$ ;

```

---

a larger value; if it is a unoccupied conference room, it will be assigned with a smaller value.

For each time step, we characterize the airflow flexibility for each zone,  $\underline{m}_t^i, \bar{m}_t^i$ , using the algorithms in (3) and (4). Let  $m_t^*$  be the dispatched total airflow of the HVAC system at time step  $t$ , we perform the following algorithm to find the ideal point for each zone

$$\max_{q_t^i} u_t^i(q_t^i) = (q_t^i)^{\alpha^i} \quad (13a)$$

$$\text{subject to: } 0 \leq q_t^i \leq 1, \quad \forall i \in \mathcal{N}, \quad (13b)$$

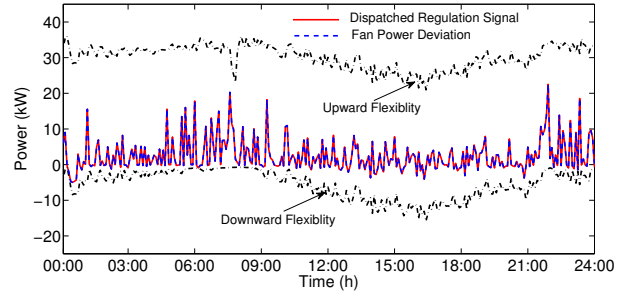
$$(q_t^j)^{\alpha^j} = d^j, \quad \forall j \neq i, \quad (13c)$$

$$(q_t^j)^{\alpha^j} \geq d^j, \quad \forall j = i, \quad (13d)$$

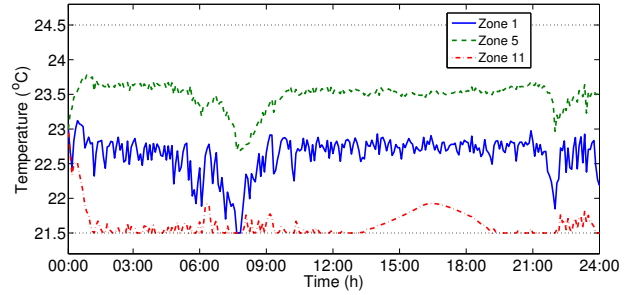
$$\sum_{i=1}^n ((\bar{m}_t^i - \underline{m}_t^i)q_t^i + \underline{m}_t^i) \leq m_t^*, \quad (13e)$$

where  $d^j$  is the disagreement point of zone  $j$  in the last negotiation iteration. We then repeat the Raiffa bargaining protocol Algorithm 3 until an  $\epsilon$  Pareto-efficient solution is achieved. We comment that the Raiffa bargaining protocol is not distributed, since it requires information from all other agents. At each step, each agent maximizes its own utility while keeping the other agents' utilities at their minimum values, which correspond to those using the disagreement points.

We next numerically compare the distributed Nash bargaining protocol (Algorithm 2) with the Raiffa bargaining protocol (Algorithm 3). In particular, the involved optimization problems (8) and (13) are solved using CVX package [28]. It is worth to mention that both protocols yield  $\epsilon$ -Pareto optimal solutions, but the computational time for the distributed Nash bargaining protocol (with initial dual variable  $\lambda_0 = 1$  and step size  $\gamma = 1$ ) is about 40 seconds, while it takes about 210 seconds for the Raiffa bargaining solution. We comment that although the initial value of the dual variable and the step size play an important role in determining the rate of convergence, the distributed Nash bargaining protocol is faster than the Raiffa bargaining protocol in general cases. Moreover, the social welfare that is defined as the Nash product with the two allocation strategies are very different. The social welfare with the Nash bargaining protocol is 0.835, which is larger than 0.686 obtained by using the Raiffa bargaining protocol. Besides comparing with



(a) Fan power deviation successfully tracks the regulation signal.



(b) Temperature trajectories of Zone 1, Zone 5, and Zone 11.

Fig. 5. Commercial building HVAC system tracks a regulation signal.

the Raiffa bargaining protocol, we also compare the Nash bargaining protocol with a proportional allocation strategy, which allocates the airflow in the following manner,

$$m_t^i = \underline{m}_t^i + \frac{\bar{m}_t^i - \underline{m}_t^i}{\sum_{j=1}^n (\bar{m}_t^j - \underline{m}_t^j)} (m_t^* - \sum_{j=1}^n \underline{m}_t^j), \quad \forall i \in \mathcal{N}.$$

However, this airflow allocation strategy yield even smaller social welfare, which is about 0.481. Moreover, it does not take each zone's preference into account.

### C. Commercial Building Balancing the Grid

In this section, we conduct numerical simulations to demonstrate commercial buildings providing frequency regulation service to the grid. Frequency regulation is one of the most important ancillary services, which is used to correct short term power imbalance between generation and load. At each time step, we first use the proposed distributed flexibility characterization method to estimate the upward and downward regulation capacities that commercial HVAC system can provide. We then construct the dispatch signal by multiplying a normalized regulation signal (which is a real regulation signal from Pennsylvania-New Jersey-Maryland Interconnection [29]) by the building's regulation capacity. To track the dispatched regulation signal, the Nash bargaining airflow allocation strategy is used to distribute the dispatched airflow to each zone. Fig. 5 shows that the fan power deviation from baseline is able to track the dispatched regulation signal very well while the temperature of each zone is strictly regulated within the pre-specified temperature band [21.5, 24.5]. Additionally, the utility functions used in the simulations are power functions (12), where the power

coefficients for the 11 zones shown in Fig. 2 are picked as [0.5, 0.5, 0.5, 0.5, 0.1, 0.1, 0.1, 0.5, 0.5, 0.5, 0.9]. We observe from Fig. 5 (b) that the larger the power coefficient a zone has, the closer its temperature trajectory is to the lower temperature bound. In particular, the average temperatures of Zone 1, Zone 5, and Zone 11 over the one-day period are respectively 22.629, 23.485, and 21.631. As a result, we see that the Nash bargaining based airflow allocation strategy respects each zone's flexibility and preference.

## VI. CONCLUSIONS AND FUTURE WORK

We studied an agent-based modeling, analysis, and control method for commercial building HVAC system to provide ancillary services to the grid. Each zone in the multi-agent-building-system was modeled as an agent or player, and we devised distributed protocols to allow them to communicate, interact, and bargain with one another locally to achieve a common global objective. A distributed flexibility characterization method was first proposed to aggregate the total power flexibility that all zones can provide to the grid. In order to track a dispatch signal, we proposed a distributed Nash bargaining protocol to allocate the airflow to each zone while respecting its preference and flexibility. Numerical experiments were conducted to compare our proposed distributed protocols with centralized approaches, and demonstrate the efficiency and scalability of our distributed protocols.

In the future, we are interested in implementing the proposed distributed flexibility characterization and resource allocation methods using VOLTTRON™, an agent-based distributed sensing and control platform developed at our Pacific Northwest National Laboratory, on a real commercial building, and evaluating its performance in field tests. A systematic study of how prediction errors of exogenous inputs such as occupancy and solar radiation impact the proposed algorithms is also desired. Another interesting direction of future research is to study a multi-agent building system and distributed coordination strategies that take various components of the HVAC system such as cooling tower, chiller, boiler, supply fan, and VAV boxes into consideration.

## REFERENCES

- [1] "Buildings energy data book." [Online]. Available: <http://buildingsdatabook.eren.doe.gov/default.aspx>
- [2] "Commercial buildings energy consumption survey: Overview of commercial buildings," Energy Information Administration, Department of Energy, Tech. Rep., December 2012.
- [3] P. Xu, P. Haves, J. E. Braun, and L. T. Hope, "Peak demand reduction from pre-cooling with zone temperature reset in an office building," in *Proceedings of ACEEE Summer Study of Energy Efficiency in Buildings*, Pacific Grove, CA, 2004.
- [4] F. Oldewurtel, A. Ulbig, M. Morari, and G. Andersson, "Building control and storage management with dynamic tariffs for shaping demand response," in *Proceedings of IEEE PES International Conference and Exhibition on Innovative Smart Grid Technologies*, 2011, pp. 1–8.
- [5] B. Kirby, "Ancillary services: Technical and commercial insights," Tech. Rep., July 2007.
- [6] H. Hao, Y. Lin, A. Kowli, P. Barooah, and S. Meyn, "Ancillary service to the grid through control of fans in commercial building HVAC systems," *IEEE Transactions on Smart Grid*, vol. 5, no. 4, pp. 2066–2074, 2014.
- [7] M. Balandat, F. Oldewurtel, M. Chen, and C. Tomlin, "Contract design for frequency regulation by aggregations of commercial buildings," in *Proceedings of Annual Allerton Conference on Communication, Control, and Computing*, Sept 2014, pp. 38–45.
- [8] J. Hughes, A. Domínguez-García, and K. Poolla, "Virtual battery models for load flexibility from commercial buildings," in *Proceedings of Hawaii International Conference on System Sciences*, Kauai, HI, 2015, pp. 2627–2635.
- [9] Y. Lin, P. Barooah, S. Meyn, and T. Middelkoop, "Experimental evaluation of frequency regulation from commercial building HVAC systems," *IEEE Transactions on Smart Grid*, vol. 6, no. 2, pp. 776–783, 2015.
- [10] W. Mai and C. Chung, "Economic MPC of aggregating commercial buildings for providing flexible power reserve," *IEEE Transactions on Power Systems*, vol. PP, no. 99, pp. 1–10, 2014.
- [11] Y. Ma and F. Borrelli, "Fast stochastic predictive control for building temperature regulation," in *Proceedings of American Control Conference*, June 2012, pp. 3075–3080.
- [12] E. Vrettos, F. Oldewurtel, F. Zhu, and G. Andersson, "Robust provision of frequency reserves by office building aggregations," in *Proceedings of the 19th IFAC World Congress*, Cape Town, South Africa, June 2014, pp. 1082–1089.
- [13] P. Zhao, G. P. Henze, M. J. Brandemuehl, V. J. Cushing, and S. Plamp, "Dynamic frequency regulation resources of commercial buildings through combined building system resources using a supervisory control methodology," *Energy and Buildings*, vol. 86, no. 2, pp. 137–150, 2015.
- [14] J. F. Nash, "The bargaining problem," *Econometrica*, vol. 18, no. 2, pp. 155–162, 1950.
- [15] Y. Lin and P. Barooah, "Issues in identification of control-oriented thermal models of zones in multi-zone buildings," in *Proceedings of IEEE Conference on Decision and Control*, 2012, pp. 6932–6937.
- [16] Y. Ma, G. Anderson, and F. Borrelli, "A distributed predictive control approach to building temperature regulation," in *Proceedings of American Control Conference*, 2011, pp. 2089–2094.
- [17] H. Hao, T. Middelkoop, P. Barooah, and S. Meyn, "How demand response from commercial buildings will provide the regulation needs of the grid," in *Proceedings of Annual Allerton Conference on Communication, Control, and Computing*, 2012, pp. 1908–1913.
- [18] ASHRAE, "The ASHRAE handbook HVAC systems and equipment (SI Edition)," 2008.
- [19] F. Oldewurtel, D. Sturzenegger, G. Andersson, M. Morari, and R. S. Smith, "Towards a standardized building assessment for demand response," in *Proceedings of IEEE Conference on Decision and Control*, 2013, pp. 7083–7088.
- [20] N. Yu, L. Tesfatsion, and C.-C. Liu, "Financial bilateral contract negotiation in wholesale electricity markets using nash bargaining theory," *IEEE Transactions on Power Systems*, vol. 27, no. 1, pp. 251–267, 2012.
- [21] G. Shrimali, A. Akella, and A. Mutapic, "Cooperative interdomain traffic engineering using nash bargaining and decomposition," *IEEE/ACM Transactions on Networking*, vol. 18, no. 2, pp. 341–352, 2010.
- [22] L. Xiao, M. Johansson, and S. P. Boyd, "Simultaneous routing and resource allocation via dual decomposition," *IEEE Transactions on Communications*, vol. 52, no. 7, pp. 1136–1144, 2004.
- [23] C. Zhao, U. Topcu, and S. H. Low, "Optimal load control via frequency measurement and neighborhood area communication," *IEEE Transactions on Power Systems*, vol. 28, no. 4, pp. 3576–3587, 2013.
- [24] L. Chen, N. Li, S. H. Low, and J. C. Doyle, "Two market models for demand response in power networks," in *Proceedings of IEEE SmartGridComm*, 2010, pp. 397–402.
- [25] A. M. Colell, "Bargaining games," in *Cooperation: Game-Theoretic Approaches*. Springer, 1997, pp. 69–90.
- [26] J. Löfberg, "Yalmip: a toolbox for modeling and optimization in MATLAB," in *Proceedings of the CACSD Conference*, Taipei, Taiwan, 2004. [Online]. Available: <http://users.isy.liu.se/johanl/yalmip>
- [27] E. Zehavi and A. Leshem, "On the allocation of multiple divisible and non-transferable commodities," *arXiv preprint arXiv:1403.7707*, 2014.
- [28] M. Grant and S. Boyd, "CVX: Matlab software for disciplined convex programming, version 2.1," <http://cvxr.com/cvx>, Mar. 2014.
- [29] "PJM regulation data." [Online]. Available: <http://www.pjm.com/markets-and-operations/ancillary-services/mkt-based-regulation/fast-response-regulation-signal.aspx>